Journal of Magnetic Resonance **137,** 437–442 (1999)
Article ID jmre.1998.1699, available online at http://www.idealibrary.com on IDEAL®

Sensitivity-Enhanced Sim-CT HMQC PFG-HBHA(CO)NH and PFG-CBCA(CO)NH Triple-Resonance Experiments

G. V. T. Swapna and Gaetano T. Montelione[1]

Center for Advanced Biotechnology and Medicine and Department of Molecular Biology and Biochemistry, Rutgers University, Piscataway, New Jersey 08854-5638

Received September 1, 1998; revised December 17, 1998

Short transverse relaxation times of C^{α} and C^{β} single-quantum coherences reduce the sensitivity of triple-resonance experiments involving transfers of C^{α}/C^{β} or H^{α}/H^{β} coherences. Multiple-quantum line-narrowing techniques improve the relaxation properties of ^{13}C coherences, thereby increasing the sensitivity of the experiment. In the present work, we describe PFG-CBCA(CO)NH and PFG-HBHA(CO)NH experiments that utilize heteronuclear multiple-quantum coherences in a simultaneous constant-time period to obtain completely decoupled spectra with improved sensitivity. Results indicate that ~30% of cross peaks show an average enhancement of ~15% in the CBCA(CO)NH experiment. In the related HBHA(CO)NH experiment, ~97% of the cross peaks show an average enhancement of ~40%.

Key Words: **protein NMR; nuclear relaxation; NMR resonance assignments; simultaneous constant-time period.**

Triple-resonance experiments provide a powerful approach for determining resonance assignments in proteins (*1–8*). However, the short transverse relaxation times of C^{α} and C^{β} single-quantum states in proteins reduce signal-to-noise ratios of these heteronuclear correlation experiments. Deuterium enrichment of the sample with deuterium decoupling during evolution of carbon magnetization is one approach for improving the transverse relaxation times of ^{13}C coherences (*9–11*). Another approach to overcoming this "short transverse relaxation problem" is to utilize heteronuclear multiple-quantum coherences (*12–19*). In these multiple-quantum states, the dominant one-bond ^{13}C–^{1}H dipolar relaxation pathway is eliminated and relevant coherences often exhibit significantly longer relaxation times.

We have recently described a simultaneous ^{1}H and ^{13}C constant-time (sim-CT) heteronuclear multiple-quantum evolution scheme which generally provides enhanced sensitivity in triple-resonance protein NMR experiments. Relative to HSQC versions, the sim-CT HMQC versions of PFG-HA(CA)(CO)NH (*19*) and (HA)CA(CO)NH (*17*) experiments were observed to have average signal-to-noise enhancements of 5–20%. In this Communication, we have applied this general approach for sensitivity enhancement in PFG-CBCA(CO)NH and PFG-HBHA(CO)NH triple-resonance experiments. Results on proteins show that the sim-CT HMQC versions of PFG-CBCA(CO)NH and PFG-HBHA(CO)NH exhibit significant signal intensity enhancements compared with the conventional HSQC versions of the same experiments.

The CBCA(CO)NH (*20–22*) and HBHA(CO)NH (*23*) protein triple-resonance experiments correlate C^{β}/C^{α} and H^{β}/H^{α} resonances of residue i, respectively, with ^{15}N and H^{N} resonances of residue $i + 1$. These pulse sequences are crucial to many general strategies for determining protein resonance assignments. Shown in Fig. 1A is a generalized schematic describing implementations of these two experiments in routine use in our laboratory. In the H^{α}/H^{β} frequency-labeled version of this experiment, transverse H^{α} and H^{β} magnetization is first frequency labeled while simultaneously developing antiphase $2H_xC_z$ magnetization, which is then converted into antiphase $2H_zC_y$ magnetization using an INEPT (*24*) coherence transfer. In the C^{α}/C^{β} frequency-labeled version of the experiment, this same antiphase $2H_zC_y$ coherence is generated without the initial proton frequency-labeling period. This $2H_zC_y$ antiphase magnetization is then refocused into $C_x^{\alpha/\beta}$ in-phase magnetization during the τfoc_{CH} delay period, while simultaneously developing antiphase $2C_y^{\alpha}C_z^{\beta}$ magnetization over the constant-time period $2T_c$. This $2C_y^{\alpha}C_z^{\beta}$ magnetization forms the basis for the ^{13}C–^{13}C COSY transfer, which is subsequently relayed through the carbonyl atom C′ to N–H_{i+1}^{N} for detection. In the case of the CBCA(CO)NH version, ^{13}C frequency labeling is developed in a constant-time fashion during the $2T_c$ period.

A serious shortcoming of this widely used triple-resonance experiment is that the C^{α} and C^{β} magnetizations are in single-quantum states throughout the relatively long $2T_c$ period, and exhibit efficient relaxation by dipolar interactions with directly bound H^{α} and H^{β} nuclei. These effects can be suppressed by utilizing multiple-quantum states during the development of the required ^{13}C–^{13}C antiphase coherences. Following concepts of simultaneous constant-time frequency evolution of multiple-quantum coherences outlined in our previous papers (*17*, *19*), we have designed and implemented sim-CT HMQC CBCA-

[1] To whom correspondence should be addressed at CABM, Rutgers University, 679 Hoes Lane, Piscataway, New Jersey 08854-5638. Fax: 732-235-4850. E-mail: guy@nmrlab.cabm.rutgers.edu.

1090-7807/99 $30.00

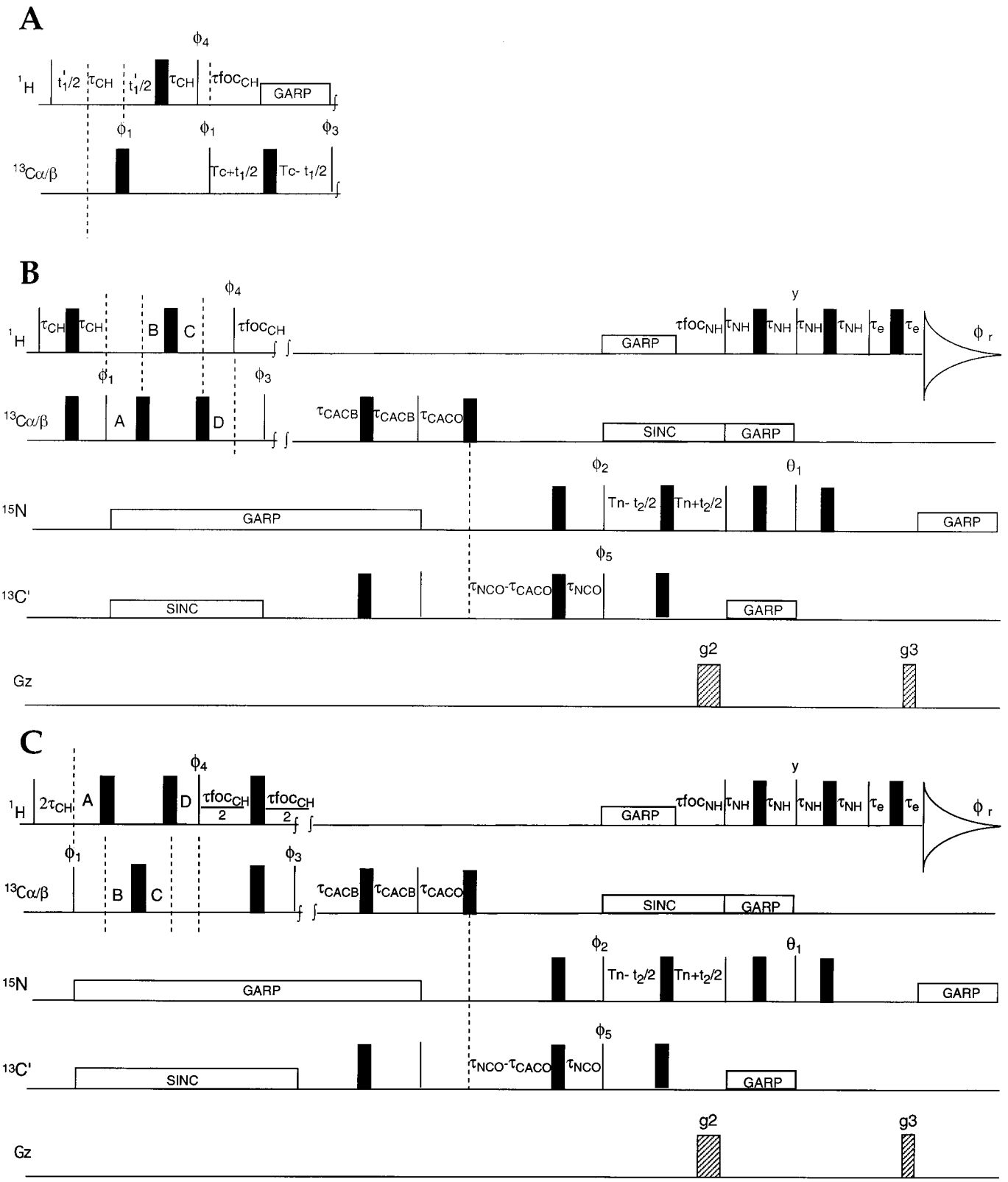

FIG. 1. Pulse sequences of 3D (A) generalized HSQC HBHACBCA(CO)NH, (B) sim-CT HMQC CBCA(CO)NH, and (C) sim-CT HMQC HBHA(CO)NH experiments. In A, $t_1' = 0$ for $^{13}C^{\alpha}$ frequency labeling while $t_1 = 0$ for $^{1}H^{\alpha}$ frequency labeling. Typical coherence transfer delays were tuned to $\tau_{CH} = 1.7$ ms, $\tau foc_{CH} = 2.15$ ms, $\tau_{CACB} = 3.25$ ms, $\tau_{CACO} = 4.8$ ms, $\tau_{NCO} = 14.5$ ms, $\tau_{NH} = 2.5$ ms, $\tau foc_{NH} = 5.4$ ms, and $\tau_e = 650$ μs, and the constant times were set to T_c

(CO)NH (Fig. 1B) and sim-CT HMQC HBHA(CO)NH (Fig. 1C) experiments that utilize multiple-quantum $2H_xC_y$ states for the development of ^{13}C–^{13}C antiphase coherence. As expected, the sim-CT HMQC versions of these experiments generally provide enhanced sensitivity compared with the corresponding conventional HSQC versions.

For both the sim-CT HMQC CBCA(CO)NH and the sim-CT HMQC HBHA(CO)NH experiments, the relevant magnetization transfer pathway up to the $^{13}C^{\beta} \rightarrow {}^{13}C^{\alpha}$ coherence transfer step (i.e., the pulse labeled with phase ϕ_3 in Figs. 1B and 1C) is described in product operator formalism (*25*) as

$$H_z^{\beta} \xrightarrow{90_x(H)} -H_y^{\beta} \xrightarrow{2\tau_{CH}} 2H_x^{\beta}C_z^{\beta} \xrightarrow{90_x(C)}$$

$$-2H_x^{\beta}C_y^{\beta} \xrightarrow{{}^1J(C^{\alpha}-C^{\beta})} 4H_x^{\beta}C_x^{\beta}C_z^{\alpha} \xrightarrow{90_y(H)}$$

$$-4H_z^{\beta}C_x^{\beta}C_z^{\alpha} \xrightarrow{\tau foc_{CH}} -2C_y^{\beta}C_z^{\alpha},$$

where H^{β}, C^{β}, and C^{α} represent angular momentum operators for $^1H^{\beta}$, $^{13}C^{\beta}$, and $^{13}C^{\alpha}$ spins, respectively. Optimal values of delays *A*, *B*, *C*, and *D* in the sim-CT HMQC CBCA(CO)NH experiment (Fig. 1B) are uniquely determined by

$$A - B - C + D + \tau foc_{CH} = t_1 \quad [1]$$

$$A + B - C - D = 0 \quad [2]$$

$$A + B + C + D + \tau foc_{CH} = 2T_c \quad [3]$$

$$A - B + C - D = 0, \quad [4]$$

where Eqs. [1]–[4] are derived from the requirements of [1] ^{13}C frequency labeling during the evolution time t_1, [2] refocusing of H^{α}/H^{β} chemical shift evolution during t_1, [3] constant-time evolution of carbon–carbon and proton–proton scalar couplings, and [4] refocusing of heteronuclear two- and three-bond scalar couplings of H^{β} and C^{β} nuclei, respectively. The solutions for this set of equations are $A = D = T_c/2 + t_1/4 - \tau foc_{CH}/2$ and $B = C = T_c/2 - t_1/4$. Similar expressions can be derived for the sim-CT HMQC HBHA(CO)NH experiment (Fig. 1C) from the requirements of H^{α}/H^{β} frequency labeling during the evolution time t_1, refocusing of ^{13}C chemical shift evolution during t_1, constant-time evolution of carbon–carbon and proton–proton scalar couplings, and refocusing of heteronuclear two- and three-bond scalar couplings of H^{β} and C^{β} nuclei, respectively; the solutions to this set of equations are $A = D = T_c/2 + t_1/4 - \tau_{CH}/2 - \tau foc_{CH}/4$ and $B = C = T_c/2 - t_1/4 + \tau_{CH}/2 - \tau foc_{CH}/4$.

These HSQC and sim-CT HMQC frequency evolution periods were compared using a uniformly ^{13}C, ^{15}N-enriched sample of bovine pancreatic trypsin inhibitor (BPTI). Representative traces along ω_1 dimensions of HSQC CBCA(CO)NH and sim-CT HMQC CBCA(CO)NH spectra recorded with identical total data collection times and resolution are shown in Fig. 2A. A similar comparison of representative ω_1 traces from HSQC HBHA(CO)NH and sim-CT HMQC HBHA(CO)NH spectra recorded, again, with identical data collection times and resolution are shown in Fig. 2B. In both sets of comparisons, many resonances exhibit significant sensitivity enhancements. For example, Cys-51 C^{β} exhibits a sim-CT HMQC:HSQC enhancement ratio of 1.32 (Fig. 2A).

A quantitative analysis of 86 well-resolved cross peaks in these CBCA(CO)NH spectra is summarized in the histogram of Fig. 2C. As in our previously described comparison of HSQC and sim-CT HMQC versions of the (HA)CA(CO)NH experiment (*17*), some cross peaks exhibit significant sensitivity enhancements, e.g., as large as 40% (Fig. 2C), while other sites exhibit lower signal intensities in the HMQC experiment compared with the conventional HSQC version. Approximately one-third of the cross peaks exhibit HMQC/HSQC enhancement factors greater than 1.0, with an average enhancement within this subset of ~15%. On the other hand, ~70% of the cross peaks exhibit HMQC/HSQC enhancement factors <1.0 with an average reduction of ~15%. The average HMQC/HSQC signal-to-noise ratio in these CBCA(CO)NH spectra is 0.93.

The transverse relaxation rates of the single-quantum $C^{\beta/\alpha}$ coherences are due mainly to dipolar relaxation of the $C^{\beta/\alpha}$ nucleus and its directly attached $H^{\beta/\alpha}$ nuclei. For methine carbons, this interaction is eliminated in the MQ coherence; for methylene carbons it is reduced. However, the dipolar interactions between these $H^{\beta/\alpha}$ nuclei and other protons that are nearby in the three-dimensional structure of the protein can

---

= 3.3 ms and T_n = 13.5 ms. The delays *A*, *B*, *C*, and *D* are set as described in the text. ^{15}N and ^{13}C spins are broadband decoupled during the periods shown using GARP (*28*). Selective $^{13}C'$ or $^{13}C^{\alpha}$ decoupling during the periods shown was done using band-selective SINC waveforms. The pulse phases are cycled as follows: $\phi_1 = +x, -x$; $\phi_2 = 8(+x), 8(-x)$; $\phi_3 = +x, -x, -x, +x, -x, +x, +x, -x, -x, +x, +x, -x, +x, -x, -x, +x$; $\phi_4 = 4(+y), 4(-y)$; $\phi_5 = +x, +x, -x, -x$; and the receiver phase $\phi_r = +x, -x, -x, +x, -x, +x, +x, -x, -x, +x, +x, -x, +x, -x, -x, +x$. All 180° pulses are applied with phase *y*, unless otherwise indicated. Quadrature detection in the t_1 dimension is obtained by changing the phase of the first 90° proton pulse for ^1H frequency labeling (A and C) or the phase of the first 180° and 90° carbon pulses for ^{13}C frequency labeling (A and B), in the States–TPPI manner (*29*), and in the t_2 domain by inverting θ_1 and the gradient g2 simultaneously as described by Kay *et al.* (*30*). Pulsed-field gradients are applied along the *z* axis with an amplitude of ~28 G/cm and gradient durations g1 and g2 of ~5 and ~0.5 ms, respectively.

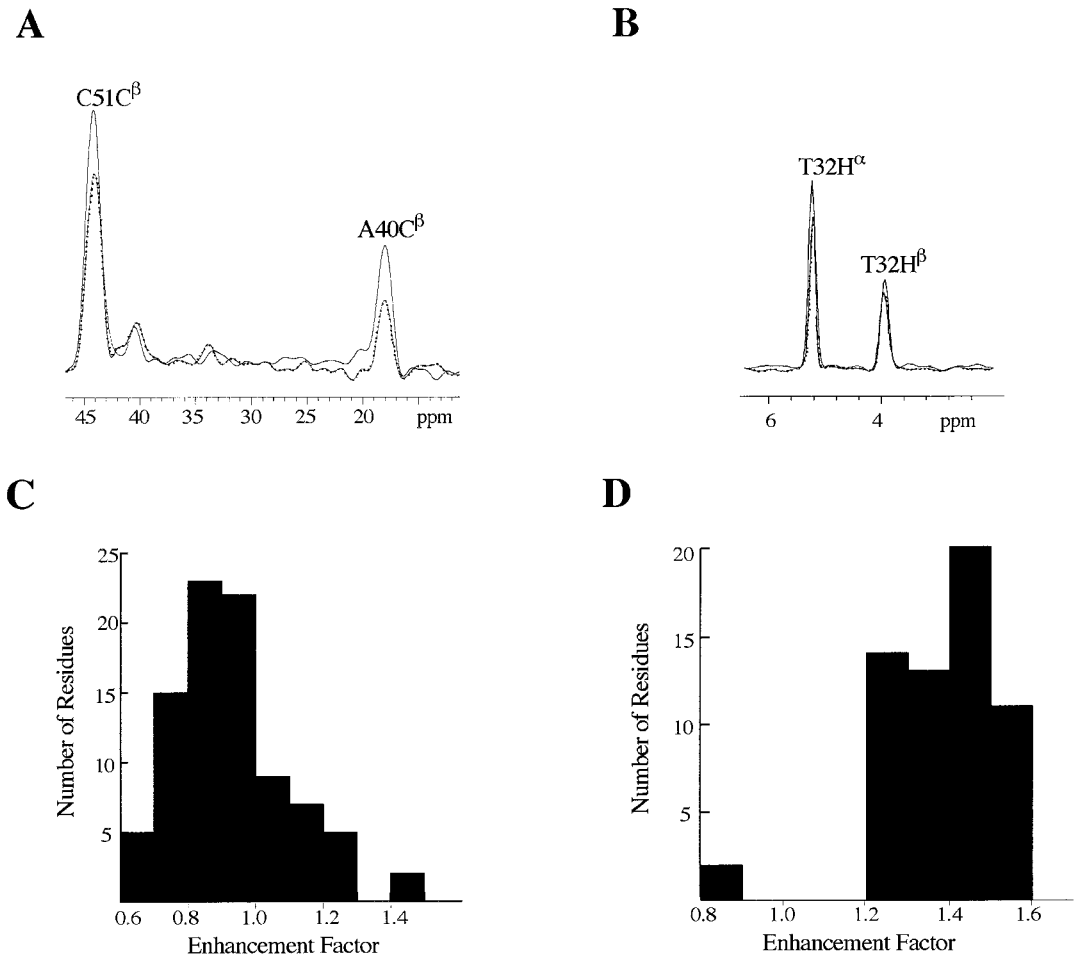

FIG. 2. Comparison of traces along ω_1 for $C^{\alpha}_{i-1}/H^{\alpha}_{i-1}(\omega_1)$–$H^{N}(\omega_3)$ cross peaks from 2D versions of CBCA(CO)NH and HBHA(CO)NH spectra. The sample was uniformly ^{13}C, ^{15}N-enriched BPTI at a concentration of 2 mM, pH 5.8, and a temperature of 20°C. These spectra were generated with the pulse sequences shown in Fig. 1 with incrementable delay $t_2 = 0$. (A) Traces from 2D spectra with frequency labeling of $^{13}C^{\alpha/\beta}$ resonances and (B) traces from 2D spectra with frequency labeling of $^{1}H^{\alpha/\beta}$ resonances. All of the 2D data sets were acquired with 42 and 1024 complex data points in t_1 and t_3, respectively, and the data in the t_1 dimension were extended to 128 complex points by linear prediction and zero-filled to 1024 points prior to Fourier transformation. The HSQC (dotted lines) and sim-CT HMQC (solid lines) spectra were recorded and processed under identical conditions and are plotted with the same vertical scale and apparent noise level. For each spectrum, 128 transients were acquired for each t_1 increment and the total collection time was ~6 h. Histogram plots of the number of cross peaks vs enhancement factor (sim-CT HMQC:HSQC intensity ratio) measured in (C) CBCA(CO)NH and (D) HBHA(CO)NH spectra of BPTI. The enhancement factor is defined as the ratio of cross-peak signal-to-average-noise ratios of the sim-CT HMQC and HSQC spectra. For these statistics, 86 well-resolved cross peaks were analyzed from the $C^{\alpha}(\omega_1)$–$H^{N}(\omega_3)$ spectra and 60 well-resolved cross peaks were analyzed from the $H^{\alpha}(\omega_1)$–$H^{N}(\omega_3)$ 2D spectra. NMR spectra were collected on a Varian Unity 500 NMR spectrometer system equipped with three independent channels and a computer-controlled fourth synthesizer for carbonyl pulses and decoupling. Protein samples were prepared in Shigemi NMR tubes. Data processing was carried out with Varian VNMR software.

contribute significantly to the transverse relaxation rates of these multiple-quantum coherences. Thus, the observed sensitivity enhancement is a balance between the improved relaxation properties of ^{1}H–^{13}C MQ coherences over SQ ^{13}C coherences due to suppression of the relaxation contribution from the directly bonded proton(s) and the effects of local proton density on ^{1}H–^{13}C MQ relaxation rates (*14, 17*); while for many $C^{\beta/\alpha}$–$H^{\beta/\alpha}$ sites in proteins the net effect is an enhanced sensitivity, for other sites the sim-CT HMQC experiment is similar to or even less sensitive than the conventional HSQC version.

Signal intensities in the sim-CT HMQC experiment are also modulated by both carbon–carbon and proton–proton homonuclear scalar-coupling interactions during the constant-time proton evolution period. Optimal values of the delay $2T_c$ determined by the set of carbon–carbon scalar couplings and relaxation effects were found to be around 8 ms. Proton–proton scalar couplings modulate the signal intensities as $\Pi_i cos(2\pi J_{HHi} T_c')$, where $2T_c' = 2T_c + 2\tau_{CH} - \tau foc_{CH}$. For an H^{β} atom of an AMX-type spin system with scalar-coupling interactions $^{3}J(H^{\alpha}$–$H^{\beta}) \sim 12$ Hz and $^{2}J(H^{\beta 2}$–$H^{\beta 3}) \sim 16$ Hz, and coherence evolution periods $2T_c = 8.4$ ms, $\tau_{CH} = 1.6$ ms, $\tau foc_{CH} = 2.3$

ms, $\Pi_i \cos(2\pi J_{HHi} T'_c) = 0.84$; i.e., the attenuation of HMQC due to proton–proton homonuclear scalar coupling can be as much as ~16%. For LONG amino acid spin systems, additional $^3J(H^\beta–H^\gamma)$ interactions can further suppress signal intensity. For many sites, these scalar-coupling effects are balanced by improved relaxation properties of the MQ coherences, resulting generally in net sensitivity enhancement.

Comparing the HSQC (Fig. 1A) and sim-CT HMQC (Fig. 1C) versions of HBHA(CO)NH, it is clear that the HSQC version of the experiment is much longer when the t_1 value is incremented for proton frequency labeling. The sim-CT HMQC experiment incorporates the proton chemical shift evolution *within* the constant-time period $2T_c$. This, together with the improved relaxation properties of MQ coherences during the evolution of $^{13}C^\alpha–^{13}C^\beta$ antiphase magnetization, results in especially large sensitivity enhancements in sim-CT HMQC HBHA(CO)NH relative to the HSQC version. A histogram summarizing these enhancements is shown in Fig. 2D; for the BPTI sample studied here ~97% of cross peaks exhibit HMQC:HSQC ratios >1.0; while the average enhancement factor for all sites is ~1.4, some sites exhibit as much as ~60% signal enhancement.

We have estimated relaxation rates for SQ ^{13}C and MQ $^{13}C–^1H$ coherences in an isolated CH_2 spin system based on theory outlined by Grzesiek and Bax (*14*). These calculations predict an enhancement in sensitivity of only about 4% (assuming $2T_c = 8.0$ ms and an isotropic correlation time τ_c of 3 ns). This is consistent with our observation that, though some $C^\beta H_2$ sites clearly exhibit significant signal enhancement in the sim-CT HMQC CBCA(CO)NH experiment, for many sites these HMQC/HSQC enhancements are minimal. In the case of the HBHA(CO)NH experiments, significantly larger HMQC/HSQC enhancement factors are observed than in the ^{13}C version. In addition to the improved relaxation properties of MQ coherences during the $2T_c$ period, in the sim-CT HMQC pulse sequence proton chemical shift evolves during the same delays used to evolve $^{13}C^\beta–^{13}C^\alpha$ antiphase coherence. This results in a shortened pulse sequence compared with the HSQC version in which ^1H frequency labeling is done prior to the polarization transfer from ^1H to ^{13}C.

We have also compared these HSQC (Fig. 1A) and sim-CT HMQC (Fig. 1C) HBHA(CO)NH experiments with a semi-constant-time HSQC (*23, 26*) version of the same experiment. For most cross peaks, intensities and signal-to-noise ratios were highest for the sim-CT HMQC version, followed by semi-constant-time HSQC, and lowest for the HSQC version.

In summary, the simultaneous ^1H and ^{13}C constant-time multiple-quantum coherence scheme described in this study has several advantages: (i) utilization of multiple-quantum coherences generally prolongs transverse relaxation times of $C^{\beta/\alpha}$ coherences; (ii) simultaneous constant-time evolution of homo- and heteronuclear couplings suppresses splittings of resonances in the indirect HMQC dimensions; and (iii) incorporation of proton frequency evolution times into the constant-time period significantly minimizes the total length of the pulse sequence. These features provide enhancement of ~40% in the sim-CT HMQC HBHA(CO)NH experiment. In the case of the sim-CT HMQC CBCA(CO)NH experiment, sensitivity enhancement is more modest and some cross peaks in fact exhibit better sensitivity in the HSQC version of the experiment. Accordingly, an optimum strategy might include running *both* HSQC and sim-CT HMQC versions of CBCA(CO)NH in order to optimize sensitivity at most sites.

The sim-CT HMQC proton evolution scheme described here significantly increases spectrum sensitivity as demonstrated in this study. Four-dimensional versions of these experiments with constant-time evolutions in three indirect dimensions can also be readily obtained without extending the pulse sequence length. Moreover, sim-CT HMQC-type experiments are expected to give even greater enhancements compared with HSQC-type experiments in larger proteins with short $^{13}C^{\beta/\alpha}$ SQ transverse relaxation times, and in partially deuterated proteins (*27*) in which deleterious $^1H–^1H$ dipolar relaxation effects are suppressed.

ACKNOWLEDGMENTS

We thank Mrs. R. Klein for useful editorial comments on the manuscript. This work was supported by grants from the National Institutes of Health (GM-50733), a New Jersey Commission on Science and Technology Research Excellence Award, and a Camille Dreyfus Teacher–Scholar Award.

REFERENCES

1. G. T. Montelione and G. Wagner, *J. Am Chem. Soc.* **111,** 5474 (1989).
2. G. T. Montelione and G. Wagner, *J. Magn. Reson.* **87,** 183 (1990).
3. M. Ikura, L. E. Kay, and A. Bax, *Biochemistry* **29,** 4659 (1990).
4. L. E. Kay, M. Ikura, R. Tschudin, and A. Bax, *J. Magn. Reson.* **89,** 496 (1990).
5. L. E. Kay, M. Ikura, and A. Bax, *J. Magn. Reson.* **91,** 84 (1991).
6. W. Boucher, E. D. Laue, S. Campbell-Burk, and P. J. Domaille, *J. Am. Chem. Soc.* **114,** 2262 (1992).
7. A. Bax and S. Grzesiek, *Acc. Chem. Res.* **26,** 131 (1993).
8. B. A. Lyons and G. T. Montelione, *J. Magn. Reson. B* **101,** 206 (1993).
9. S. Grzesiek, J. Anglister, H. Ren, and A. Bax, *J. Am. Chem. Soc.* **115,** 4369 (1993).
10. T. Yamazaki, W. Lee, M. Revington, D. L. Mattiello, F. W. Dahlquist, C. H. Arrowsmith, and L. E. Kay, *J. Am. Chem. Soc.* **116,** 6464 (1994).
11. B. T. Farmer II and R. A. Venters, *J. Am. Chem. Soc.* **117,** 4187 (1995).
12. R. R. Ernst, G. Bodenhausen, and A. Wokaun, "Principles of Nuclear Magnetic Resonance in One and Two Dimensions," Clarendon Press, Oxford, United Kingdom (1987).
13. M. Billeter, D. Neri, G. Otting, T. Q. Qian, and K. Wüthrich, *J. Biomol. NMR* **2,** 257 (1992).
14. S. Grzesiek and A. Bax, *J. Biomol. NMR* **6,** 335 (1995).
15. S. Grzesiek, H. Kuboniwa, A. P. Hinck, and A. Bax, *J. Am. Chem. Soc.* **117,** 5312 (1995).

16. R. H. Griffey and A. G. Redfield, *Q. Rev. Biophys.* **19,** 51 (1987).
17. G. V. T. Swapna, C. B. Rios, Z. Shang, and G. T. Montelione, *J. Biomol. NMR* **9,** 105 (1997).
18. J. P. Marino, J. L. Diener, P. B. Moore, and C. Griesinger, *J Am. Chem. Soc.* **119,** 7361 (1997).
19. Z. Shang, G. V. T. Swapna, C. B. Rios, and G. T. Montelione, *J Am. Chem. Soc.* **119,** 9274 (1997).
20. S. Grzesiek and A. Bax, *J. Am. Chem. Soc.* **114,** 6291 (1992).
21. D. R. Muhandiram and L. E. Kay, *J. Magn. Reson. B* **103,** 203 (1994).
22. C. B. Rios, W. Feng, M. Tashiro, Z. Shang, and G. T. Montelione, *J. Biomol. NMR* **8,** 345 (1996).
23. S. Grzesiek and A. Bax, *J. Biomol. NMR* **3,** 185 (1993).
24. G. A. Morris and R. Freeman, *J. Am. Chem. Soc.* **101,** 760 (1979).
25. O. W. Sørensen, G. W. Eich, M. H. Levitt, G. Bodenhausen, and R. R. Ernst, *Prog. NMR Spectrosc.* **16,** 163 (1983).
26. T. M. Logan, E. T. Olejniczak, R. X. Xu, and S. W. Fesik, *J. Biomol. NMR* **3,** 225 (1993).
27. R. M. Gschwind, G. Gemmecker, and H. Kessler, *J. Biomol. NMR* **11,** 191 (1998).
28. A. J. Shaka, P. B. Barker, and R. Freeman, *J. Magn. Reson.* **64,** 547 (1984).
29. D. Marion, M. Ikura, R. Tschudin, and A. Bax, *J. Magn. Reson.* **84,** 393 (1989).
30. L. E. Kay, P. Keifer, and T. Saarinen, *J. Am. Chem. Soc.* **114,** 10663 (1992).